Dalton
Transactions

ROYAL SOCIETY
OF CHEMISTRY

COMMUNICATION

View Article Online
View Journal

Check for updates

Cite this: DOI: 10.1039/d1dt02121d

Received 25th June 2021,
Accepted 19th July 2021

DOI: 10.1039/d1dt02121d

rsc.li/dalton

Bifunctional zinc and magnesium Schiff-base complexes containing quaternary ammonium side-arms for epoxide/CO_2 coupling reactions†

Arnut Virachotikul,[a] Nattiya Laiwattanapaisarn,[a] Kittipong Chainok[b] and Khamphee Phomphrai *[a,c]

Novel bifunctional zinc and magnesium Schiff-base complexes containing quaternary ammonium halide side-arms were developed. Zinc complex 1Et-I (0.02 mol%) having an iodide anion has shown the highest TOF for the propylene oxide/CO_2 coupling reaction of up to 459 h^{-1}. This TOF value was maintained even when the catalyst loading was reduced to 0.005 mol%.

Carbon dioxide utilization has gained much interest over the past decades by converting CO_2 into various value-added products including methanol,[1] carboxylic acids,[2–4] ureas,[5] polycarbonates,[6–8] and cyclic carbonates.[9–12] In particular, because cyclic carbonates have high boiling points, high polarity, and high flash points, they can be used in various applications as polar aprotic solvents,[13] electrolytes,[11] and starting materials for polymer synthesis.[14] In general, CO_2 is considered as an attractive C1 source due to its abundance, inexpensiveness, and renewability.[15–17] Many catalyst systems have been developed ranging from ionic salts,[18] organocatalysts,[10,19] and metal complexes[20–26] for epoxide/CO_2 coupling reactions. In many metal catalyst systems, especially porphyrin- and salen-based complexes, the use of cocatalysts such as quaternary ammonium salts (TBA^+X^-) is typically required to obtain outstanding activity by driving the reaction through the bicomponent pathway. However, the combination of a catalyst and cocatalyst, called a binary system, suffered from activity drop at a low catalyst loading. To solve this problem, bifunctional catalyst systems have been developed by tethering a cocatalyst onto the ligand framework in the complex.[27–34] However, compared to bifunctional metal(III) catalysts, the development of metal(II) bifunctional systems was very limited with only a few examples of tethering catalysts supported by porphyrin[35,36] and salen-based ligands.[37,38] In 2012, Sakai and coworkers reported bifunctional zinc and magnesium porphyrin catalysts that showed outstanding activities for the coupling of 1,2-epoxyhexane (EH) and CO_2 with a TOF of up to 12 000 h^{-1} which is the highest value for a metal(II) catalyst for the epoxide/CO_2 coupling reaction.[35] In 2014, bifunctional zinc(salpyr) complexes having a pyridinium halide moiety on the ligand backbone were developed by Kleij and coworkers.[37] These catalysts demonstrated promising activities for the selective production of various cyclic carbonates. Among various ligated metal complexes, Schiff-base metal complexes have received our attention because of their promising catalytic activities in various chemical reactions, structural diversity, ease of synthesis, and systematic modification.[39–41] Herein, bifunctional zinc and magnesium Schiff-base complexes containing quaternary ammonium halide side-arms were developed and used for epoxide/CO_2 coupling reactions.

The Schiff-base ligand framework can be synthesized easily by the reaction of substituted salicylaldehyde and *N*,*N*-diethylethylenediamine. Quaternary ammonium halides can then be incorporated into the ligand framework through a simple reaction of alkyl halides (R–X) with the corresponding Schiff-base ligands having diethylamino side-arms (see Scheme 1 and the ESI†). While there are a few reports on the synthesis and structures of zinc complexes having $-NHR_2X$ moieties (X = halides),[38,42–44] there is no report on Schiff-base zinc complexes having an $-NR_3X$ attachment as reported in this work. In this study, we focused on five aspects of catalyst modifications for the effects of (1) the alkyl group R, (2) the anion X, (3) the C=N imine or C–N amine backbone, (4) the side-arm length, and (5) the metal center as presented in Scheme 1. Zinc and magnesium complexes can be synthesized by the

---

[a] *Department of Materials Science and Engineering, School of Molecular Science and Engineering, Vidyasirimedhi Institute of Science and Technology (VISTEC), Wangchan, Rayong 21210, Thailand. E-mail: khamphee.p@vistec.ac.th*

[b] *Materials and Textile Technology, Faculty of Science and Technology, Thammasat University, Khlong Luang, Pathum Thani 12121, Thailand*

[c] *Research Network of NANOTEC-VISTEC on Nanotechnology for Energy, Vidyasirimedhi Institute of Science and Technology, Wangchan, Rayong 21210, Thailand*

† Electronic supplementary information (ESI) available: Experimental details, ^1H and ^{13}C NMR of all compounds, and X-ray structures. CCDC 2090817 (**6**). For ESI and crystallographic data in CIF or other electronic format see DOI: 10.1039/d1dt02121d

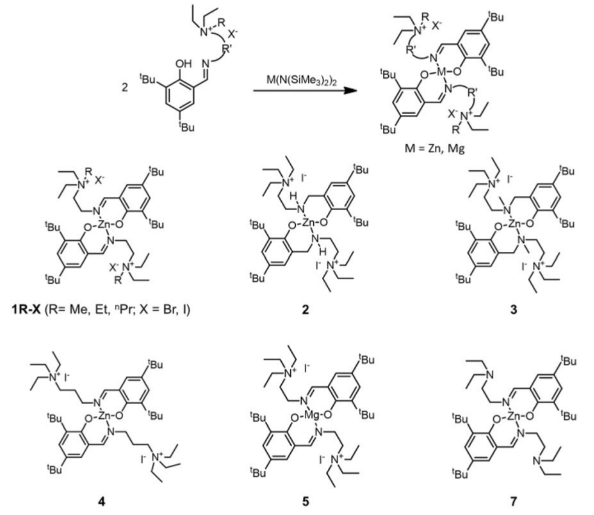

Scheme 1 The synthetic procedure and structures of the bifunctional Schiff-base metal complexes used in this work.

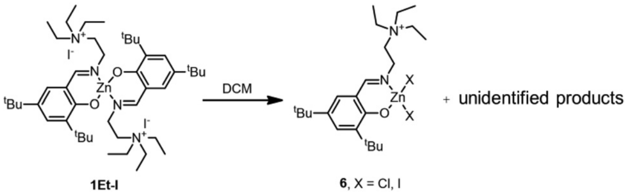

Scheme 2 Decomposition of complex **1Et-I** in concentrated DCM into complex **6**.

reaction of $M[N(SiMe_3)_2]_2$ (M = Zn, Mg) with the corresponding ligands. Homoleptic metal complexes (L_2M) were targeted because they are usually more stable compared to the heteroleptic complexes (LMX) that could undergo the Schlenk equilibrium from LMX to L_2M and MX_2. Metal complexes **1–5** were successfully synthesized in moderate to high yields. The MALDI-TOF mass spectra of all complexes demonstrated isotopic patterns corresponding to their cationic species having one halide anion (see the ESI, Fig. S33–S40†). The structural analysis of the complexes was carried out using single-crystal X-ray crystallography. After several attempts, only the recrystallization of complex **1Et-I** in toluene gave crystals that are suitable for X-ray data collection. Unfortunately, the quality of the crystals is insufficient for structural refinement. Therefore, only qualitative information could be extracted from this structure. The crystal structure revealed the expected zinc complex having a distorted tetrahedron geometry of the zinc center showing the available space above the $O1^i$–Zn–O1 pocket suitable for substrate coordination (Fig. 1). The two iodide anions stay close to the ammonium side-arm and do not coordinate with the zinc metal. While complex **1Et-I** was stable in chloroform or toluene, we found that it decomposed slowly into complex **6** during recrystallization only in concentrated dichloromethane as shown in Scheme 2 giving crystals that are suitable for X-ray crystallography. Surprisingly, the crystal structure revealed one zinc atom attached to one ligand and two chlorine atoms (Fig. 2). The substitution disorder of chlorine and iodine atoms was observed in the crystal structure with chlorine as a majority (92.5%) and iodine as a minority (7.5%). The complex decomposition is possibly a result of the substitution reaction of iodide with dichloromethane generating a chloride anion in the solution. This substitution reaction only occurred in the less crowded dichloromethane but not in chloroform. The strong Zn–Cl interaction could also facilitate the formation of decomposed product **6** (Scheme 2). It should be noted that this process only occurred in a concentrated dichloromethane solution of **1Et-I** during recrystallization and no decomposition was observed during the complex synthesis and storage in the solid state or in other solvents. The concentration-dependent generation of zinc ammonium complexes was previously reported by Wu, which showed that the ammonium zinc halide complex is preferred at a high concentration.[45]

All complexes were tested for their activities for the coupling reaction of propylene oxide (PO) and CO_2 using a PO : catalyst ratio of 2000 : 1 (0.05 mol% catalyst) under neat conditions with a CO_2 pressure of 100 psi at 75 °C for 6 h giving propylene carbonate (PC) as a product exclusively. Firstly, the effect of the quaternary ammonium size was investigated since the ionic strength between the ammonium group

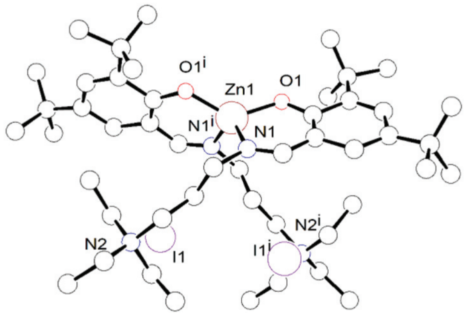

Fig. 1 PLUTO drawing of **1Et-I**. Hydrogen atoms are omitted for clarity.

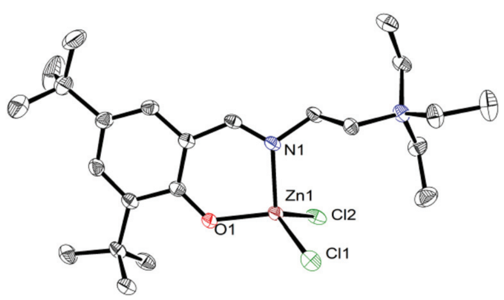

Fig. 2 X-ray crystal structure of complex **6** with thermal ellipsoids drawn at the 50% probability level. Solvent molecules and hydrogen atoms are omitted for clarity. Selected bond distances (Å) and angles (°): O1–Zn1 1.929(1), N1–Zn1 2.031(1), Zn1–Cl1 2.298(1), Zn1–Cl2 2.308(1); O1–Zn1–N1 93.9(1), O1–Zn1–Cl1 119.4(1), O1–Zn1–Cl2 112.6(1), N1–Zn1–Cl1 103.4(1), N1–Zn1–Cl2 112.6(1), Cl1–Zn1–Cl2 110.6(1).

Table 1 PO and CO_2 coupling reaction using Schiff-base complexes containing quaternary ammonium side-arms[a]

Entry	Catalyst	T (°C)	P_{CO_2} (psi)	Conv.[b] (%)	TON[c]	TOF[d] (h^{-1})
1	**1Me-I**	75	100	32	640	107
2	**1Et-I**	75	100	49	980	163
3	**1Pr-I**	75	100	30	600	100
4	**1Et-Br**	75	100	7	140	23
5	**2**	75	100	47	940	157
6	**3**	75	100	24	480	80
7	**4**	75	100	33	660	110
8	**5**	75	100	20	400	67
9	**7**	75	100	Trace	—	—
10[e]	**7**	75	100	13	260	43
11[f]	$\mathbf{HL^1_{Et\text{-}I}}$	75	100	1.3	13	2.2
12	**1Et-I**	100	100	77	1540	257
13	**1Et-I**	100	300	86	1720	287

[a] Reaction conditions: PO (2.0 mL), PO : catalyst ratio = 2000 : 1, 6 h. [b] Determined by ^{1}H-NMR spectroscopy. [c] TON = (monomer : catalyst ratio) × %conversion/100. [d] TOF = TON/time (h). [e] 2.0 equiv. of TBAI were added into the reaction mixture. [f] 2.0 equiv. of the catalyst were used.

and halide has a strong influence on the nucleophilicity of the halide (Table 1, entries 1–3). Complex **1Et-I** shows a higher TOF of 163 h^{-1} compared to **1Me-I** (TOF = 107 h^{-1}) and **1Pr-I** (TOF = 100 h^{-1}), respectively. A small ammonium size of **1Me-I** could lead to a strong interaction between the ammonium group and iodide, making iodide a poorer nucleophile compared to **1Et-I** and **1Pr-I**. In contrast, **1Pr-I** has a weaker ammonium-halide ion pair, but the bulkiness of the large quaternary ammonium group can also obstruct the reaction. Therefore, the ethyl group could be a good balance between the effects of the ion pair strength and bulkiness of the ammonium moiety.

The effect of the anion was also studied by comparison of **1Et-I** and **1Et-Br**. In this reaction, the anion plays two important roles as both an initiator in the epoxide ring-opening step and a leaving group in the cyclization step. By changing iodide to bromide, the nucleophilicity of the halide anion improved but a trade off was observed with a lower leaving ability. From the results, the activity of complex **1Et-Br** (23 h^{-1}) is significantly lower than that of **1Et-I** (163 h^{-1}) possibly due to the better leaving ability of iodide in the cyclization step (Table 1, entry 4). The reduced derivatives (complex **2** having a C–N–H moiety and complex **3** having a C–N–Me moiety, Table 1 entries 5 and 6, respectively) were also tested in comparison with **1Et-I** (having a C═N moiety). The main difference of the amine group compared to the imine moiety is the flexibility of the ligand structure that allows the optimum transition state in the reaction, thus decreasing the activation barrier. However, the better electron-donating ability of amine results in a less Lewis acidic metal center which could decrease the epoxide coordination/activation. Complex **2** (TOF = 157 h^{-1}) is slightly less active compared to **1Et-I** (TOF = 163 h^{-1}). However, the activity of **3** (TOF = 80 h^{-1}) is significantly lower presumably as a result of the steric hindrance of methyl groups on the amine around the zinc center.

A previous report showed that the distance between the anion and metal center has a strong effect on the catalytic activity. Therefore, there is an optimum distance to exhibit the highest performance.[36] For example, higher energy is required for a halide anion to reach the backside of the epoxide for a short side-arm while for a longer side-arm, the activity is limited by the long distance between the anion and the active site. To investigate the effect of the side-arm length, complex **4** having a $-(CH_2)_3-$ side-arm was tested in the reaction giving a TOF of 110 h^{-1} (entry 7) which is lower than that of **1Et-I** having a $-(CH_2)_2-$ side-arm. In addition to zinc, the magnesium complex is also a promising catalyst for the epoxide/CO_2 coupling reaction. However, the activity of **5** (M = Mg, TOF = 67 h^{-1}) is significantly lower than that of **1Et-I** (M = Zn, TOF = 163 h^{-1}). The higher Lewis acidity of Mg could result in the formation of stable magnesium carbonate species that limits the cyclization step.

To confirm the vital role of the ammonium halide side-arm, complex **7** having only an $-NEt_2$ side-arm was synthesized and tested for its activity. Only a trace amount of PC was obtained indicating the necessity of the cocatalyst in the binary system (Table 1, entry 9). The combination of complex **7** and 2 equiv. of tetrabutylammonium iodide (TBAI) as the binary counterpart can facilitate the coupling reaction giving a TOF value of 43 h^{-1} (entry 10) but still significantly lower than the bifunctional system using **1Et-I**. To demonstrate if the Schiff-base ligand containing a quaternary ammonium side-arm could also act as an organocatalyst for the coupling reaction,[46] the reaction using only two equivalents of free ligand **HL1Et-I** (the ligand used to form complex **1Et-I**) was carried out and only 1.3% conversion of PO was observed (Table 1, entry 11). It is conclusive that throughout the catalyst screening process, complex **1Et-I** shows the highest activity compared to its derivatives and its binary counterpart. The effect of solvents was also studied by adding dimethylformamide (DMF), toluene, tetrahydrofuran (THF), and dichloromethane (DCM) into the reaction (see ESI, Table S1†). In all cases, the activities dropped giving TOF values of 157, 140, 97, and 27 h^{-1}, respectively. The lowest activity in DCM could presumably result from the slow decomposition of **1Et-I** into complex **6** during the coupling reaction. At a higher temperature (100 °C), the activity can be improved to 257 h^{-1} (Table 1, entry 12). Furthermore, when the reaction was conducted at a higher CO_2 pressure of 300 psi, a very high conversion of PO with a significantly higher TOF of 287 h^{-1} (Table 1, entry 13) was achieved. Because the tethered quaternary ammonium side-arm will always bring the iodide counterion close to the metal center in the bifunctional system, the activity of the catalyst should be retained at a low catalyst loading. To demonstrate the vital role of the bifunctional concept in this system, the equivalents of PO were increased from 5000, 10 000, and 20 000 at 100 °C and 300 psi CO_2 (Fig. 3). Complex **1Et-I** still exhibited a very high TOF of approximately 450 h^{-1} even at a low catalyst loading of 0.005 mol% showing the advantage of the bifunctional concept of this system. To observe the reaction profile, a plot between the TON and reaction time using a

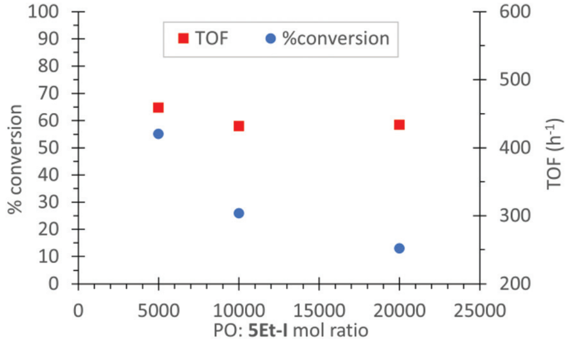

Fig. 3 Conversion of PO and TOF values at different PO : **1Et-I** ratios at T = 100 °C, P = 300 psi CO_2, 6 h.

PO : **1Et-I** molar ratio of 10 000 : 1 reveals the continuous increase of the TON when the reaction time was prolonged to 48 h indicating the durability of **1Et-I** (see the ESI, Fig. S41†).

In addition to PO, various epoxides including terminal epoxides and internal epoxides were applied in this catalyst system. Complex **1Et-I** can catalytically convert these epoxides into the corresponding cyclic carbonates with TOF values ranging from 1.7 to 275 h^{-1} (Fig. 4). The TOF values of terminal epoxides are significantly higher than those of internal epoxides because of the lower steric hindrance on the methylene position compared to the methine position for internal epoxides. In some catalyst systems, a mixture of cyclic carbonates and polycarbonates was observed when internal epoxides were used.[47–50] However, no polycarbonates were observed for both cyclopentene oxide and cyclohexene oxide indicating the high chemoselectivity of this catalyst system for cyclic carbonate production.

In summary, bifunctional Schiff-base zinc and magnesium complexes with quaternary ammonium halide side-arms were successfully synthesized, characterized, and used as bifunctional catalysts for the synthesis of cyclic carbonates *via* epoxide/CO_2 coupling reactions. From the catalyst screening, complex **1Et-I** was proven to be the best catalyst in this series for the coupling reaction of PO and CO_2 with a TOF of up to 459 h^{-1}. The TOF values still maintain at this value even when the epoxide : catalyst molar ratios were increased to 20 000 equivalents (0.005 catalyst mol%). In addition, this catalyst system can be applied to other external and internal epoxides for the selective production of cyclic carbonates.

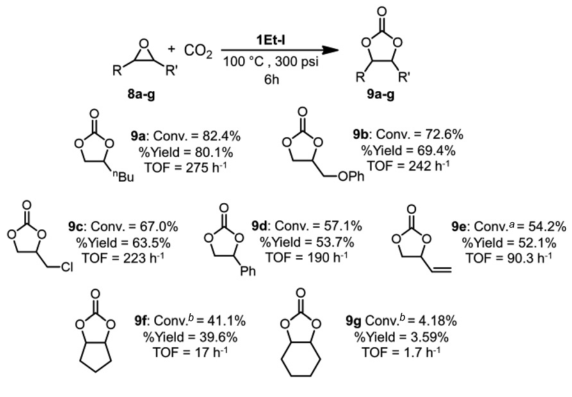

Fig. 4 Conversion, isolated yield, and TOF of different epoxides using epoxide (2.0 mL), epoxide : **1Et-I** ratio = 2000 : 1, 100 °C, CO_2 = 300 psi, t = 6 h; %conversion was determined by ^{1}H-NMR spectroscopy by comparison of the integrals of the corresponding cyclic carbonates and epoxides of the crude sample. ^{a} t = 12 h. ^{b} t = 48 h.

Author contributions

Arnut Virachotikul: conceptualization, investigation, visualization, formal analysis, and writing-original draft; Nattiya Laiwattanapaisarn: investigation and formal analysis; Kittipong Chainok: formal analysis and validation; and Khamphee Phomphrai: conceptualization, validation, editing, and supervision.

Conflicts of interest

There are no conflicts to declare.

Acknowledgements

The authors acknowledge financial support from the Vidyasirimedhi Institute of Science and Technology (VISTEC). Support of the scientific instrument by Frontier Research Center, Vidyasirimedhi Institute of Science and Technology, is gratefully acknowledged. This work has been partially supported by the NANOTEC, NSTDA, Ministry of Science and Technology, through its program of Research Network NANOTEC.

Notes and references

1 I. U. Din, M. S. Shaharun, M. A. Alotaibi, A. I. Alharthi and A. Naeem, *J. CO_2 Util.*, 2019, **34**, 20–33.
2 A. Correa and R. Martin, *Angew. Chem., Int. Ed.*, 2009, **48**, 6201–6204.
3 S.-S. Yan, Q. Fu, L.-L. Liao, G.-Q. Sun, J.-H. Ye, L. Gong, Y.-Z. Bo-Xue and D.-G. Yu, *Coord. Chem. Rev.*, 2018, **374**, 439–463.
4 S. N. Riduan and Y. Zhang, *Dalton Trans.*, 2010, **39**, 3347–3357.
5 N. W. Krase and V. L. Gaddy, *J. Ind. Eng. Chem.*, 1922, **14**, 611–615.
6 M. Taherimehr and P. P. Pescarmona, *J. Appl. Polym. Sci.*, 2014, **131**, 41141.
7 Y. Xu, L. Lin, M. Xiao, S. Wang, A. T. Smith, L. Sun and Y. Meng, *Prog. Polym. Sci.*, 2018, **80**, 163–182.
8 G. Trott, P. K. Saini and C. K. Williams, *Philos. Trans. R. Soc., A*, 2016, **374**, 20150085.

9 M. North, R. Pasquale and C. Young, *Green Chem.*, 2010, **12**, 1514–1539.

10 M. Cokoja, M. E. Wilhelm, M. H. Anthofer, W. A. Herrmann and F. E. Kuhn, *ChemSusChem*, 2015, **8**, 2436–2454.

11 T. Sakakura and K. Kohno, *Chem. Commun.*, 2009, 1312–1330.

12 X. Jin, J. Ding, Q. Xia, G. Zhang, C. Yang, J. Shen, B. Subramaniam and R. V. Chaudhari, *J. CO_2 Util.*, 2019, **34**, 115–148.

13 B. Schäffner, F. Schäffner, S. P. Verevkin and A. Börner, *Chem. Rev.*, 2010, **110**, 4554–4581.

14 G. Rokicki, *Prog. Polym. Sci.*, 2000, **25**, 259–342.

15 H. Arakawa, M. Aresta, J. N. Armor, M. A. Barteau, E. J. Beckman, A. T. Bell, J. E. Bercaw, C. Creutz, E. Dinjus, D. A. Dixon, K. Domen, D. L. DuBois, J. Eckert, E. Fujita, D. H. Gibson, W. A. Goddard, D. W. Goodman, J. Keller, G. J. Kubas, H. H. Kung, J. E. Lyons, L. E. Manzer, T. J. Marks, K. Morokuma, K. M. Nicholas, R. Periana, L. Que, J. Rostrup-Nielson, W. M. H. Sachtler, L. D. Schmidt, A. Sen, G. A. Somorjai, P. C. Stair, B. R. Stults and W. Tumas, *Chem. Rev.*, 2001, **101**, 953–996.

16 T. Sakakura, J.-C. Choi and H. Yasuda, *Chem. Rev.*, 2007, **107**, 2365–2387.

17 M. Mikkelsen, M. Jørgensen and F. C. Krebs, *Energy Environ. Sci.*, 2010, **3**, 43–81.

18 J. Ma, J. Liu, Z. Zhang and B. Han, *Green Chem.*, 2012, **14**, 2410.

19 D.-H. Lan, N. Fan, Y. Wang, X. Gao, P. Zhang, L. Chen, C.-T. Au and S.-F. Yin, *Chin. J. Catal.*, 2016, **37**, 826–845.

20 H. Buttner, L. Longwitz, J. Steinbauer, C. Wulf and T. Werner, *Top. Curr. Chem.*, 2017, **375**, 50.

21 M. North, *ARKIVOC*, 2012, **2012**, 610.

22 J. W. Comerford, I. D. V. Ingram, M. North and X. Wu, *Green Chem.*, 2015, **17**, 1966–1987.

23 K. Kiatkittipong, M. A. A. Mohamad Shukri, W. Kiatkittipong, J. W. Lim, P. L. Show, M. K. Lam and S. Assabumrungrat, *Processes*, 2020, **8**, 548.

24 A. Decortes, A. M. Castilla and A. W. Kleij, *Angew. Chem., Int. Ed.*, 2010, **49**, 9822–9837.

25 N. Laiwattanapaisarn, A. Virachotikul and K. Phomphrai, *Dalton Trans.*, 2021, DOI: 10.1039/D1DT01903A.

26 M. Strianese, D. Pappalardo, M. Mazzeo, M. Lamberti and C. Pellecchia, *Dalton Trans.*, 2020, **49**, 16533–16550.

27 X. Zhang, Y.-B. Jia, X.-B. Lu, B. Li, H. Wang and L.-C. Sun, *Tetrahedron Lett.*, 2008, **49**, 6589–6592.

28 M. North, P. Villuendas and C. Young, *Chemistry*, 2009, **15**, 11454–11457.

29 W. M. Ren, Y. Liu and X. B. Lu, *J. Org. Chem.*, 2014, **79**, 9771–9777.

30 T. Chang, L. Jin and H. Jing, *ChemCatChem*, 2009, **1**, 379–383.

31 C. X. Miao, J. Q. Wang, Y. Wu, Y. Du and L. N. He, *ChemSusChem*, 2008, **1**, 236–241.

32 R. Luo, X. Zhou, S. Chen, Y. Li, L. Zhou and H. Ji, *Green Chem.*, 2014, **16**, 1496–1506.

33 J. Martinez, F. de la Cruz-Martinez, M. A. Gaona, E. Pinilla-Penalver, J. Fernandez-Baeza, A. M. Rodriguez, J. A. Castro-Osma, A. Otero and A. Lara-Sanchez, *Inorg. Chem.*, 2019, **58**, 3396–3408.

34 J. Melendez, M. North and P. Villuendas, *Chem. Commun.*, 2009, 2577–2579.

35 T. Ema, Y. Miyazaki, S. Koyama, Y. Yano and T. Sakai, *Chem. Commun.*, 2012, **48**, 4489–4491.

36 T. Ema, Y. Miyazaki, J. Shimonishi, C. Maeda and J. Y. Hasegawa, *J. Am. Chem. Soc.*, 2014, **136**, 15270–15279.

37 C. Martín, C. J. Whiteoak, E. Martin, M. Martínez Belmonte, E. C. Escudero-Adán and A. W. Kleij, *Catal. Sci. Technol.*, 2014, **4**, 1615–1621.

38 X.-D. Lang, Y.-C. Yu and L.-N. He, *J. Mol. Catal. A: Chem.*, 2016, **420**, 208–215.

39 K. C. Gupta and A. K. Sutar, *Coord. Chem. Rev.*, 2008, **252**, 1420–1450.

40 W. Al Zoubi and Y. G. Ko, *J. Organomet. Chem.*, 2016, **822**, 173–188.

41 X. Liu, C. Manzur, N. Novoa, S. Celedón, D. Carrillo and J.-R. Hamon, *Coord. Chem. Rev.*, 2018, **357**, 144–172.

42 T. Chattopadhyay, M. Mukherjee, K. S. Banu, A. Banerjee, E. Suresh, E. Zangrando and D. Das, *J. Coord. Chem.*, 2009, **62**, 967–979.

43 X.-W. Zhu, Z.-G. Yin, X.-Z. Yang, G.-S. Li and C.-X. Zhang, *Acta Crystallogr., Sect. E: Struct. Rep. Online*, 2009, **65**, m1293–m1294.

44 J.-Y. Li, *Acta Crystallogr., Sect. E: Struct. Rep. Online*, 2009, **65**, m1611.

45 H. W. Chiang, Y. T. Su and J. Y. Wu, *Dalton Trans.*, 2013, **42**, 15169–15182.

46 M. Hong, Y. Kim, H. Kim, H. J. Cho, M. H. Baik and Y. Kim, *J. Org. Chem.*, 2018, **83**, 9370–9380.

47 D. J. Darensbourg and D. R. Billodeaux, *Inorg. Chem.*, 2005, **44**, 1433–1442.

48 J. A. Castro-Osma, K. J. Lamb and M. North, *ACS Catal.*, 2016, **6**, 5012–5025.

49 F. D. Monica, B. Maity, T. Pehl, A. Buonerba, A. De Nisi, M. Monari, A. Grassi, B. Rieger, L. Cavallo and C. Capacchione, *ACS Catal.*, 2018, **8**, 6882–6893.

50 J. Kiriratnikom, N. Laiwattanapaisarn, K. Vongnam, N. Thavornsin, P. Sae-Ung, S. Kaeothip, A. Euapermkiati, S. Namuangruk and K. Phomphrai, *Inorg. Chem.*, 2021, **60**, 6147–6151.